NANO LETTERS

2007
Vol. 7, No. 1
161−166

Nanoscale Cell Adhesion Ligand Presentation Regulates Nonviral Gene Delivery and Expression

Hyun Joon Kong,[†,‡] Susan Hsiong,[†,§] and David J. Mooney*[,†]

Division of Engineering and Applied Science, Harvard University, Cambridge, Massachusetts 02138, Department of Chemical and Biomolecular Engineering, University of Illinois, Urbana, Illinois 61801, and Department of Chemical Engineering, University of Michigan, Ann Arbor, Michigan 49105

Received October 23, 2006; Revised Manuscript Received November 23, 2006

ABSTRACT

It is hypothesized that the nanoscale organization of cell adhesion ligands in a synthetic ECM regulates nonviral gene delivery. This hypothesis was examined with pre-osteoblasts cultured on substrates which present varied density and spacing of synthetic adhesion ligands. The levels of gene transfer and expression were increased with the density of adhesion ligands, but decreased with the spacing of ligands, due to changes in the cell growth rate. This study provides a material-based control point on the nanometer scale for nonviral gene based therapies.

Nonviral gene vectors [e.g., plasmid DNA (pDNA)] are being increasingly used in a variety of therapeutic applications[1−3] because of safety concerns related to viral vectors.[4] One of the major challenges with the use of nonviral gene vectors is the very limited range of transgene expression level, owing to the poor efficiency of gene transfer.[5] Therefore, there have been extensive efforts to design novel gene carriers to improve the levels of gene transfer and expression using lipids, polycations, dendrimers, nanorods, and oligopeptides[5−7] and efforts to spatially concentrate the pDNA.[8] In contrast, the design of gene delivery systems has largely ignored the importance of the cellular microenvironment in gene uptake and expression, although target tissues for in vivo gene delivery present varying cellular microenvironments.

Gene transfer is related to the rate of cell proliferation,[9] and the chemistry and mechanics of the ECM to which a cell adheres regulates many aspects of cell phenotype, including proliferation, apoptosis, and differentiation.[10−14] These findings suggest that alteration of the ECM may allow one to regulate a cell's ability to take up and express exogeneous genes. Recently, we have demonstrated that the mechanical rigidity of synthetic ECM used as adhesion substrates plays a critical role in modulating gene transfer and expression.[15] In this study, we demonstrate a new material-based control point to regulate nonviral delivery by engineering the nanoscale organization of cell adhesion molecules in the synthetic ECM. The underlying mechanism of this regulation appears to be related to the material control over cell proliferation. The spatial distribution of cell adhesion molecules at the nanometer scale was controlled using a gel matrix formed from cross-linked alginate molecules containing covalently bound synthetic oligopeptides containing the Arg-Gly-Asp (RGD) sequence (RGD peptides) which mediate cell adhesion.[16] Because unmodified alginate molecules are highly inert to cell adhesion and protein adsorption,[17] cellular adhesion to gels functionalized with RGD peptides is solely attributed to the bonding between cell receptors and RGD peptides.

The overall density of RGD peptides (N_{RGD}) and the distance between islands of RGD peptides (d_{RGD}), which are known to regulate cell proliferation,[11] were used as variables to control the spatial organization of RGD peptides. N_{RGD} was varied from 3×10^9 to 60×10^9 mm^{-2} by altering the degree of substitution, defined as the number of RGD peptides bound to a single polymer chain (Figure 1a). The area occupied by a single polymer chain modified with RGD peptides was defined as an island of RGD peptides. Analysis with gel permeation chromatography showed that the degree of substitution had little influence on the radius of gyration of the polymer chains, inferring a minimal change in the size of islands of RGD peptides and the distance between them (d_{RGD}) with varying degree of substitution. d_{RGD} was varied from 36 to 120 nm, at a given N_{RGD} of 6×10^9 mm^{-2}, by diluting RGD peptide-modified polymer chains with unmodified polymer chains in the gel matrix (Figure 1d). d_{RGD} was

* Corresponding author. Telephone: (617) 384-9624. Fax: (617) 495-2800. E-mail: mooneyd@deas.harvard.edu.
[†] Division of Engineering and Applied Science, Harvard University.
[‡] Department of Chemical and Biomolecular Engineering, University of Illinois.
[§] Department of Chemical Engineering, University of Michigan.

10.1021/nl062485g CCC: $37.00
Published on Web 12/08/2006

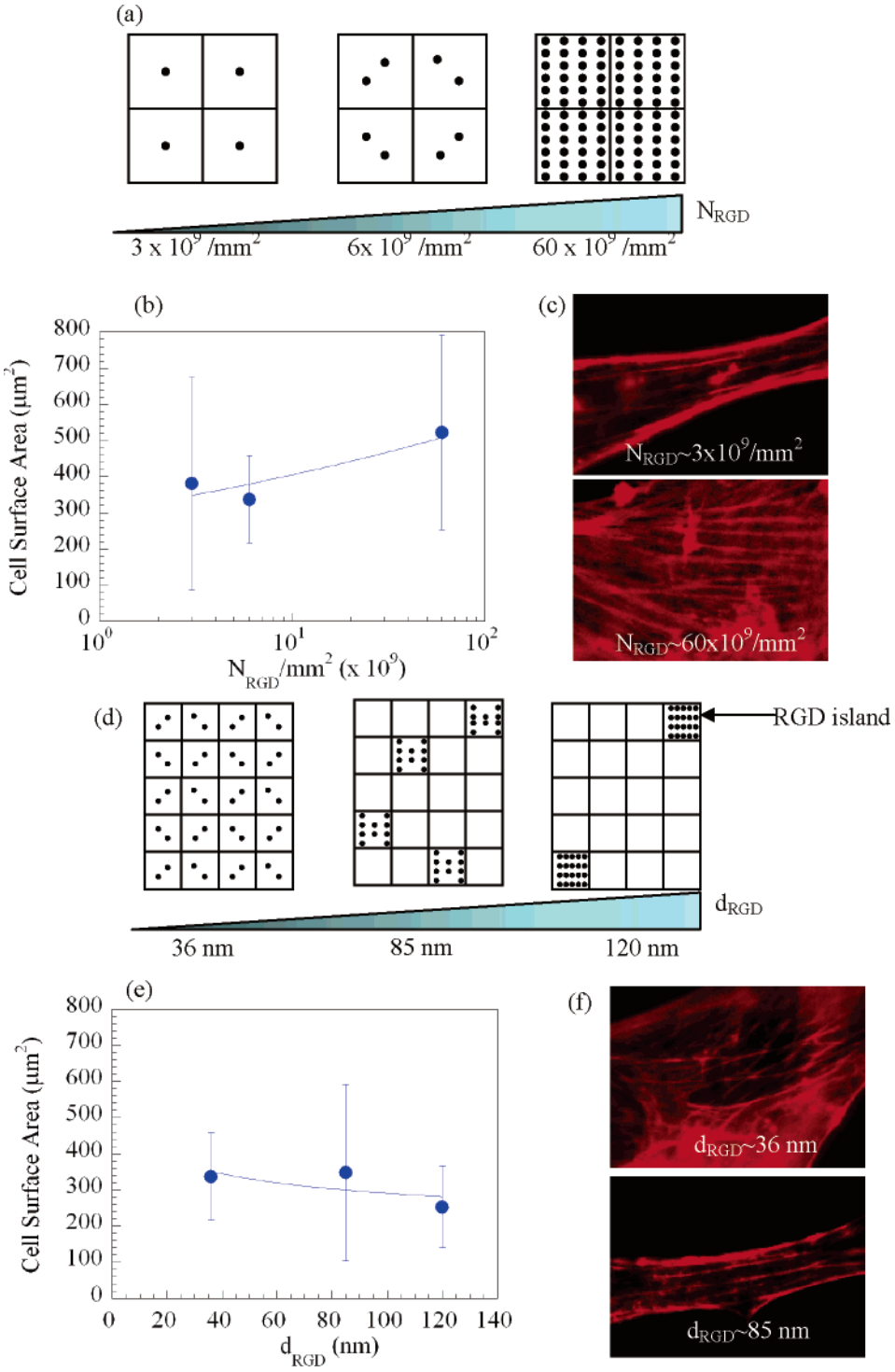

Figure 1. Schematic illustration of nanoscale spatial organization of RGD peptides in the gel matrix to which a cell adheres, and its influence on cell adhesion. Total density of RGD peptides (N_{RGD}) was varied from 3×10^9 to 6×10^9 and 60×10^9 mm^{-2} (a) using polymer molecules with different degree of substitution of RGD peptides. N_{RGD} did not significantly alter the surface area of cells adhered to the gel matrix (b), but enhanced the formation of intracellular actin stress fibers (labeled with rhodamine phalloidin) (c). The distance between RGD islands (d_{RGD}) was varied from 36 to 85 and 120 nm (d) by diluting RGD peptide-modified polymer molecules with unmodified polymer molecules. The increase in d_{RGD} at a given N_{RGD} of 6×10^9 mm^{-2} did not significantly change the surface area of cells (e), but limited formation of stress fibers (f). Each grid in the illustration represents an island of RGD peptides with a scale of 30 nm by 30 nm. ● in grid represents RGD peptides bound to polymer chain. Data points and error bars in parts b and e represent the mean and standard deviation from more than 10 cells at each condition.

calculated with a Monte Carlo simulation based on a nonoverlapping random percolation model.[18] Increasing the dilution ratio leads to larger d_{RGD}, and the number of RGD peptides in an one island was raised in parallel from 2 to 20 to maintain a constant N_{RGD}. These variations in the spatial organization of RGD peptides had minimal influences on the physical properties of gel matrix (i.e., elastic modulus and swelling ratio) or on the interaction between the gel and gene vectors.

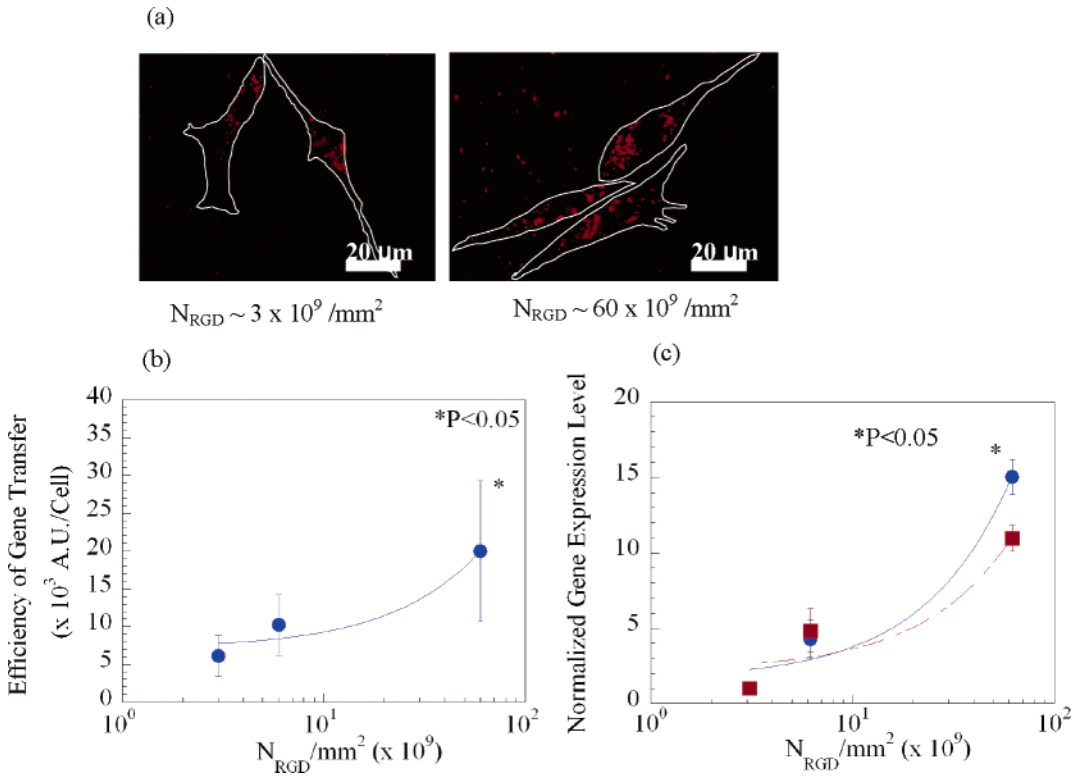

Figure 2. Gene delivery regulated with the total density of RGD peptides (N_{RGD}) presented from the gel matrix to which cells adhered. Microscopic images show the increases in the cellular uptake of the rhodamine-labeled pDNA condensates with N_{RGD} (a). White lines in photomicrographs represent the border of cells adhered to the gel matrix. The efficiency of gene transfer, quantified from the photomicrographs, linearly increased with N_{RGD} ($R^2 = 0.94$) (b). The gene expression level (● in part c) and the gene expression level normalized to the average surface area of cells (■ in part c) also linearly increased with N_{RGD} ($R^2 = 0.94$). More than 20 cells at each condition were used for the quantitative analysis of the efficiency of gene transfer. Differences in the values in parts b and c for cells adhered to gels with the highest N_{RGD} vs the two other conditions were statistically significant ($p < 0.05$). The gene expression level in part c was normalized to the gene expression level attained from cells cultured on gels with N_{RGD} of 3×10^9 mm^{-2}. Data points and error bars represent the mean and standard deviation from four independent experiments.

We first examined whether these material variables modulate the adhesion of preosteoblasts to the gel matrix, as this can significantly influence cell fate.[11] The dependency of the extent of cell spreading, quantified with the surface area of cells on N_{RGD}, was statistically insignificant, although the average values were increased with N_{RGD} (Figure 1b). In contrast, the number of stress fibers formed in a single cell was increased with N_{RGD} (Figure 1c). The variation in d_{RGD} at a given N_{RGD} had a statistically insignificant influence on the cell morphology, although the average values were decreased with increasing d_{RGD} (Figure 1e). However, increases in d_{RGD} significantly limited the formation of stress fibers (Figure 1f). These results suggest that both N_{RGD} and d_{RGD} mediate cytoskeletal rearrangements, which have been related to signaling pathways promoting cell proliferation.[19]

Next, the role of N_{RGD} in gene therapy was examined by quantifying the efficiency of gene transfer and expression level in cells adhered to gel matrices presenting different N_{RGD}. pDNA encoding for the luciferase protein was condensed with poly(ethyleneimine) (PEI) to yield nanosize pDNA condensates with enhanced cellular uptake, and delivered to cells.[20] Interestingly, the efficiency of gene transfer quantified using pDNA labeled with rhodamine was significantly enhanced with N_{RGD}, as illustrated with the linear increase in the fluorescence yield per cell (Figure 2a,b). Subsequently, the gene expression level was quantified from the luciferase activity in the cells, and this linearly increased with N_{RGD} (Figure 2c). The gene expression level normalized to the average surface area of cells was also linearly related to N_{RGD}.

Manipulation of d_{RGD} also modulated nonviral gene delivery, even as N_{RGD} remained constant. Increasing d_{RGD} linearly decreased the cellular uptake of pDNA condensates, as verified by quantifying the fluorescence yield per cell (Figure 3a,b). Both overall gene expression levels and expression levels normalized to the average surface area of cells exponentially decreased with d_{RGD} [gene expression level $\propto \exp(-2d_{RGD})$] (Figure 3c). This inverse relationship between the gene expression level and d_{RGD} was also found with cells maintained in 3D culture (cells encapsulated in the gel matrix) (Figure 3d), although the magnitude of this effect was more evident with the larger d_{RGD}.

The relation between ECM control over gene delivery and cell growth was next assessed by quantifying ^{3}H thymidine incorporation, as ^{3}H thymidine is incorporated by cells synthesizing DNA. The magnitude of cell growth increased with N_{RGD} (Figure 4a), and, inversely, the magnitude of cell growth decreased with d_{RGD} (Figure 4b), as expected from past studies. Directly monitoring cell growth by quantifying cell number over time confirmed these effects of N_{RGD} and

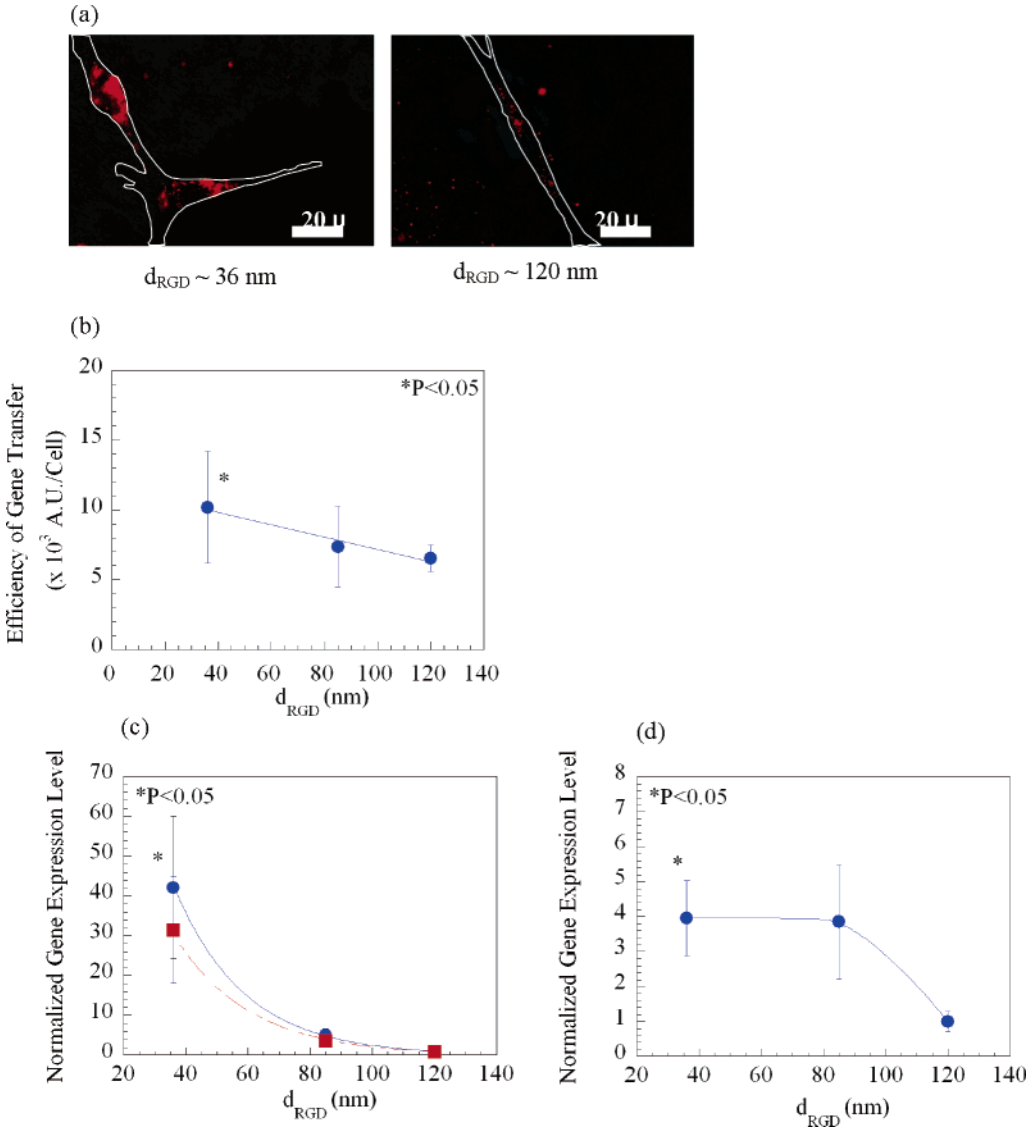

Figure 3. Gene delivery regulated with the distance between islands of RGD peptides (d_{RGD}), as the total density of RGD peptides was kept constant at 6×10^9 mm^{-2}. Microscopic images show the decrease in the cellular uptake of the rhodamine-labeled pDNA condensates with d_{RGD} (a). White lines in photomicrographs represent borders of cells adhered to the gel matrix. The efficiency of gene transfer quantified from photomicrographs was linearly decreased with d_{RGD} ($R^2 = 0.96$) (b). The gene expression level (● in part c) and the gene expression level normalized to the average surface area of cells (■ in part c) exponentially decreased with d_{RGD} ($R^2 = 1$). Increasing d_{RGD} also down-regulated the gene expression level in cells cultured within the 3D gel matrix (d). Differences in the values in part b for cells cultured on gels presenting the largest d_{RGD} (~120 nm) vs those on gels presenting the smallest d_{RGD} (~36 nm) were statistically significant ($p < 0.05$). The gene expression levels in parts c and d were normalized to the value attained from cells cultured on gels presenting d_{RGD} of 120 nm. Data points and error bars represent the mean and standard deviation from four independent experiments.

d_{RGD} on proliferation (data not shown). Both the efficiency of gene transfer (data not shown) and gene expression levels correlated in an exponential fashion to cell growth (Figure 4c), although the dependency of gene expression on cell growth was distinct for the two material variables.

Altogether, the results of this study demonstrate that the nanoscale organization of RGD peptides allows one to regulate nonviral gene delivery to both cells adhered to 2D substrates and those encapsulated in 3D matrices. Both N_{RGD} and d_{RGD} likely modulated the cell cycle by mediating cytoskeletal rearrangements and activation of intracellular signaling pathways.[19] No significant influence of surface area of cells on the gene delivery and expression was observed over the range examined in these studies. Manipulation of cell mitosis may directly alter the cellular uptake of exogeneous genes and the resultant gene expression level, as cell division has been previously noted to facilitate the entry of pDNA into cells.[9] It is likely that the greater dependency of the gene expression level on d_{RGD} in 2D vs 3D cell culture is related to the decreased frequency of cell cycle progression in 3D. However, it is unclear whether the decreased proliferation is inherent to 3D culture generally, or if it relates to the ability of cells in 2D culture to spread more extensively than cells in this 3D culture, and more broadly probe their environment. One interesting finding from the current study is that the magnitude of the dependency of gene expression levels on the material variables was larger than the dependency of the efficiency of gene transfer on N_{RGD} and d_{RGD}.

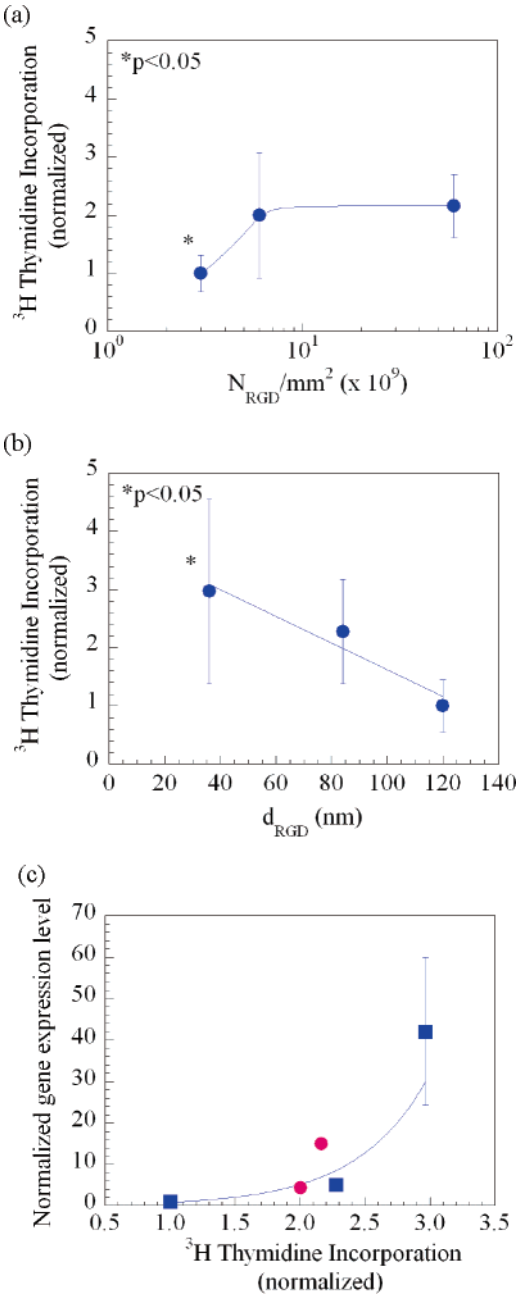

Figure 4. Spatial organization of RGD peptides regulated the rate of cell proliferation, which was quantified with ^{3}H thymidine incorporation. The amount of DNA synthesis was increased proportional to N_{RGD} (a) or with the inverse of d_{RGD} (b). Hence, the extent of cell proliferation was related to the normalized gene expression level following an exponential curve (c) ($R^2 = 0.94$). In part a, differences in the values for cells cultured on the gel matrix presenting the smallest N_{RGD} vs the two other conditions were statistically significant ($p < 0.05$). In part b, differences in the values for cells cultured on the gel matrix presenting the smallest d_{RGD} vs the two other conditions were also statistically significant ($p < 0.05$). Data points and error bars represent the mean and standard deviation from four independent experiments. In part c, curves -●- and -■- represent conditions in which N_{RGD} and d_{RGD}, respectively, were varied.

However, this result infers that material signals further influence events beyond pDNA uptake, and these additional control points may include the intracellular dissociation of pDNA condensates, their escape from lysosomes, and/or their trafficking to the cell nucleus.[7] However, this issue must be further examined, as the dependencies of the efficiency of gene transfer and expression level on N_{RGD} and d_{RGD} may also relate to the different analytical methods used in their evaluation.

This study demonstrates for the first time that the number and nanoscale distribution of cell adhesion molecules in a material play critical roles in nonviral gene delivery. This is a previously undescribed material-based control point for gene transfer, and may significantly contribute to improving the quality of various gene-based therapies. We envisage that these results can be reproduced with diverse types of cells, including primary cells, and other biomaterials functionalized to promote cell adhesion.[21] The results of this study may also be relevant to understand the varying degrees of gene transfer in cells within tissues under different conditions (e.g., normal vs pathologic ECM), as diseases and the state of development may alter the assembly and organization of the ECM.[22] In these situations, the concepts learned from this study may be useful in predicting the efficacy of gene transfer in a known ECM environment, and also in recreating, in vitro, more realistic tissue models to study these processes.[23] Most current model systems simply involve coating adhesion substrates with cell adhesion molecules, without regard to the critical effects of ligand presentation. Furthermore, the results of this study may be used to guide the design of gene activated matrices,[24] in which localized gene therapy is promoted in vivo by the migration of cells into a plasmid DNA-loaded material.[3] Proper ligand presentation in the material may be used to stimulate cell proliferation and subsequently promote the local and extended expression of target therapeutic molecules from both endogeneous and transplanted cells.

Acknowledgment. The authors thank the NIH/NIDCR (R 37 DE013033) and US Army Research Laboratories and Research Office (DAAD-19-03-1-0168) for financial support of this research.

Supporting Information Available: Text giving a description of the experimental procedures. This material is available free of charge via the Internet at http://pubs.acs.org.

References

(1) Glover, D. J.; Lipps, H. J.; Jans, D. A. *Nat. Rev. Gene* **2005**, *6*, 299.
(2) Niidome, T.; Huang, L. *Gene Ther.* **2002**, *9*, 1647.
(3) Huang, Y. C.; Kaigler, D.; Rice, K. G.; Krebsbach, P. H.; Mooney, D. J. *J. Bone Mineral Res.* **2005**, *20*, 848.
(4) Cavazzana-Calvo, M.; Lagresle, C.; Hacein-Bey-Abina, S.; Fischer, S.A. *Annu. Rev. Med.* **2005**, *56*, 585.
(5) Mastrobattista, E.; van der Aa, M. A. E. M.; Hennink, W. E.; Crommelin, D. J. A. *Nat. Rev. Drug Discovery* **2006**, *5*, 115.
(6) Park, T. G.; Jeong, J. H.; Kim, S. W. *Adv. Drug Deliv. Rev.* **2006**, *58*, 467.
(7) Pack, D. W.; Hoffman, A. S.; Pun, S.; Stayton, P. S. *Nat. Rev. Drug Discovery* **2005**, *4*, 581.
(8) Segura, T.; Shea, L. D. *Bioconjugate Chem.* **2002**, *13*, 621.
(9) Fasbender, A.; Zabner, J.; Zeiher, B. G.; Welsh, M. J. *Gene Ther.* **1997**, *4*, 1173.
(10) Discher, D. E.; Jammey, P.; Wang, Y. L. *Science* **2005**, *310*, 1139.
(11) Lee, K. Y.; Alsberg, E.; Hsiong, S.; Comisar, W.; Linderman, J.; Ziff, R.; Mooney, D. J. *Nano Lett.* **2004**, *4*, 1501.

(12) Keselowsky, B. G.; Collard, D. M.; Garcia, A. *Proc. Natl. Acad. Sci U.S.A.* **2005**, *102*, 5953.
(13) Koo, L. Y.; Irvine, D. J.; Mayes, A. M.; Lauffenburger, D. A.; Griffith, L. G. *J. Cell Sci.* **2002**, *115*, 1423.
(14) Kong, H. J.; Polte, T. R.; Alsberg, E.; Mooney, D. J. *Proc. Natl. Acad. Sci. U.S.A.* **2005**, *102*, 4300.
(15) Kong, H. J.; Liu, J.; Riddle, K.; Matsumoto, T.; Leach, K.; Mooney, D. J. *Nat. Mater* **2005**, *4*, 460.
(16) Rowley, J.; Mooney, D. J. *J. Biomed. Mater. Res.* **2002**, *60*, 217.
(17) Smetana, K. *Biomaterials* **1993**, *14*, 1046.
(18) Comisar, W. A.; Hsiong, S.; Kong, H. J.; Mooney, D. J.; Linderman, J. J. *Biomaterials* **2006**, *27*, 2322.
(19) Cai, S.; Pestic-Dragovich, L.; O'Donnell, M. E.; Wang, N.; Ingber, D.; Elson, E.; De, Lanerolle, P. *Am. J. Physiol.-Cell Physiol.* **1998**, *275*, C1345.
(20) Boussif, O.; Lezoualch, F.; Zanta, M. A.; Mergny, M. D.; Scherman, D.; Demeneix, B.; Behr, J. P. *Proc. Natl. Acad. Sci. U.S.A.* **1995**, *92*, 7297.
(21) Hersel, U.; Dahmen, C.; Kessler, H. *Biomaterials* **2003**, *23*, 4385.
(22) Ingber, D. E. *Ann. Med.* **2003**, *35*, 564.
(23) Griffith, L. G.; Swartz, M. A. *Nat. Rev. Mol. Cell Biol.* **2006**, *7*, 211.
(24) Bonadio, J. *Adv. Drug Deliv. Rev.* **2000**, *44*, 185.

NL062485G